ORIGINAL ARTICLE

Assessment of aquifer properties, protectivity and corrosivity using resistivity method: a case study of Federal College of Education (Technical), Omoku

D. O. Okoroh[1,2] · J. C. Ibuot[1,2]

Abstract

Geohydraulic properties are important in describing the behaviour and variability of aquifer units. The aquifer properties, protectivity, and corrosivity were assessed using an electrical resistivity technique within the campus of the Federal College of Education (Technical), Omoku, and its environs. The electrical resistivity technique employed the Schlumberger electrode configuration with vertical electrical sounding (VES) within a maximum current electrode separation of 400 m. Interpretation of the VES result revealed four geo-electrical layers constrained by borehole lithology logs as motley topsoil, medium-grained sand, fine-medium grained sand, and gravelly sand. The first order geo-electric indices (bulk aquifer resistivity, thickness, and pore-water resistivity) were used to estimate the geohydraulic parameters. Formation factor (0.43–4.57), effective porosity (0.24–1.13), hydraulic conductivity (0.0001–7.4027 m/day), transmissivity (0.0019–225.7824 m²/day), longitudinal conductance (0.0048–0.1022 Ω^{-1}), and transverse resistance (1549.40–20710.30 Ωm^2) aid in appraising the groundwater repositories. The corrosivity rating of the top soil varies from 66.67% practically non-corrosive (PNC), 16.67% moderately corrosive (MC), and 16.67% slightly corrosive (SC). The entire study area was delineated as having poor aquifer protective capacity, which showed that the area is susceptible to contamination.

Keywords Groundwater · VES · Geo-electric layers · Protective capacity · Resistivity

Introduction

The Niger-delta region of Nigeria is under serious and increasing pressure not only due to the expanding population but also to the increasing activities of the oil and gas exploration industries. The exploration activities of the oil and gas industries have greatly affected the surface water in most of the Niger-delta region of Nigeria. As such, assessing the water is difficult since most of the surface water is contaminated as a result of oil spillage on both water and land. Groundwater is an important resource that is used for drinking water, irrigation, and industrial processes. However,

groundwater can easily become contaminated by pollutants from agricultural, industrial, and residential sources. Additionally, groundwater can become depleted if it is overused or if there is a prolonged drought (Ibanga & George, 2016; Omeje et al., 2023). Groundwater, unlike phreatic water or soil moisture, occurs in the saturated zone of the subsurface. Since alternative water sources are unreliable and expensive to develop, groundwater provides a reliable option to meet the ever-increasing demand of the rural populace. Man relies greatly on groundwater for his daily water needs since it requires minor water treatment to make it potable. The underlying aquifer can be contaminated as a result of inappropriate or uncontrolled activities at the land surface, which include the disposal of waste and spillage of chemicals. The quality of groundwater is continuously aggravated by increasing pressure from pollution as a result of widespread vulnerability to contamination from spilled hydrocarbons and leachates arising from indiscriminate surface disposal of wastes (Abam & Nwankwoala, 2020). Groundwater availability depends largely upon the subsurface and surface geology as well as climate, porosity and permeability

✉ J. C. Ibuot
johnson.ibuot@unn.edu.ng

1 Department of Physics, School of Education Science, Federal College of Education (Technical), Omoku, Rivers State, Nigeria

2 Department of Physics and Astronomy, University of Nigeria, Nsukka, Enugu State, Nigeria

of a geologic formation, which controls its ability to hold and transmit water through the aquifer layers (George et al., 2022). Groundwater occurs in an aquifer which is a geologic formation capable of storing and transmitting sufficient quantity of water necessary for human survival and economic development (Bricker et al., 2017; Nugraha et al., 2021). Aquifer repositories provide a dependable water supply option that can meet the water needs of a community. According to literatures on the earth's subsurface, it acts as a natural filter through a process called natural attenuation. When water or other substances pass through soil and rock layers, the layers act as a physical and chemical barrier that can remove impurities and pollutants (George et al., 2014; Obiora et al., 2016).

Factors such as the depth to the water table and materials overlying the aquifer layers influence an aquifer's vulnerability. According to researchers (Akpan et al., 2013; Ekanem et al., 2021; George et al., 2014; Ibuot et al., 2019a; Nugraha et al. 2021), increased permeability of rocks leads to increased percolation and infiltration of surface pollutants into the subsurface aquifer. Many authors (Abiola et al., 2009; Adeniji et al., 2014; Bayewu et al., 2018; Ekanem et al., 2021; Ibuot et al., 2017a, 2019b; Mogaji et al., 2011; Obiora et al., 2015; Thomas et al., 2020) have investigated the protective capacity and vulnerability of groundwater repositories. When hazardous chemicals are intentionally disposed of, accidentally spilled, or applied to the ground for agricultural purposes, they percolate through the subsurface, and when they eventually reach the groundwater repositories, they can contaminate its potability and pose a serious threat to public health.

Permeability, porosity, and overburden thickness of a geologic formation control the rate of groundwater contamination (Ibuot et al., 2017b; Obiora et al., 2015). The surface pollutants infiltrating the subsurface depend on the nature of the geologic materials that overlie the aquifer units and lead to polluting plumes. Since the earth's layers act as natural filters for percolating fluids, groundwater is usually available, clean, and bereft of contaminants or pollutants (Ibuot et al., 2017b; Umar & Igwe, 2019). The purification of water as it flows through the voids is enhanced by the sluggish flow of groundwater through the subsurface. The permeability and thickness of the protective layers determine the protectivity (protective capacity) of the aquifers and the ease of fluid flow through the subsurface (Obiora & Ibuot, 2020). Groundwater can flow through pores, fissures, and fractures in rocks and carry with it dissolved pollutants as it percolates through the subsurface strata. The flow of groundwater through the subsurface is controlled by the nature of the subsurface geological composition (Bashir et al., 2014; George et al., 2015) and gravity. The nature of the subsurface materials is an important factor to consider in any hydrogeologic environment, since its properties and variations are the goals

of hydrogeologic and hydrogeophysical investigations (Daniel et al., 2022; Opara et al., 2020).

The indiscriminate disposal of waste (poor waste management) enhances the deterioration of groundwater quality since leachates that are formed from dumpsites, sewage from latrines, leakage from pipes, and oil spillage percolate through the covering layers of the subsurface into the hydrogeologic units (Hossain et al., 2014; Oseji et al., 2018; Umar & Igwe, 2019). Different chemical substances are leached into the aquifer units and their concentrations can change the chemistry of groundwater, thus altering the potability of groundwater. The water can also be corrosive if the geomaterials contain more corrosive-enhancing substances. In groundwater exploration, the water is pumped to the surface through pipes, and these pipes can be affected by corrosion if the subsurface geomaterial is corrosive. Corrosivity is a geologic hazard that can cause lead and copper in pipes to leach into drinking water and cause leaks in plumbing. The degree of corrosivity varies depending on the conductivity of the geomaterials.

The electrical resistivity method has been employed in different locations and by different researchers (Adeniji et al., 2014; Aleke et al., 2018; George, 2020; Ibanga & George, 2016; Ibuot & Obiora, 2021; Ibuot et al., 2022; Lahjouj et al., 2020; Putranto et al., 2018) in appraising the hydrogeological conditions of the heterogeneous earth subsurface. These include mapping of saturated hydrogeologic layers from the adjoining formations, groundwater potential, aquifer vulnerability, assessment of the infiltration rate of the vadose zone, groundwater contamination studies, and flow unit analysis. Due to the resistivity contrast observed in the zone of saturation, the resistivity method is preferred to other geophysical methods since the variation of resistivity/conductivity of the argillites is displayed vertically and horizontally (Loke, 2009; 2015; Obiora et al., 2018). The electrical resistivity method utilizes vertical electrical sounding (VES) to investigate the variations of subsurface geologic materials. The study area has witnessed the decline in the quality of surface water, loss of aquatic life, and land due to environmental pollution resulting from oil exploration. Consequently, one of the major challenges of the residents of the area is that of ensuring potable water in adequate amounts to meet the needs of the growing human population. Most of the aquifers in the area are usually exploited without any assessment of the aquifer's protectivity against contamination or the quality of the groundwater. Also, there is no available information about the corrosivity of the subsurface layers. This study is motivated by these situations to enhance the development of an effective and sustainable groundwater management scheme to evade any outbreak of water-borne diseases in the area. The aim of this study is, therefore, to use the surface electrical resistivity method to investigate the subsurface properties to assess

the protectivity and corrosivity of aquifer units and also the variability of these properties.

Location and geological setting of the study area

The Federal College of Education (Technical), Omoku, lies between latitudes 5.33° N and 5.35° N, and longitudes 6.63° E and 6.66° E (Fig. 1) and is located in the coastal town of Omoku in Rivers State, Nigeria. Because of its rich oil and gas deposits, the community is home to the Nigerian Agip Oil Company (NAOC), and other multinational oil companies operating in the community. It is also a central business hub of the Orashi region of the Rivers State of Nigeria (Tamunobereton-ari et al., 2014). The study area lies within the Niger Delta Basin, which is underlain by the Benin Formation, Agbada Formation, and Akata Formation. The Akata Formation, which is mainly shale and clay, and the Agbada Formation, which is generally fluviatile and fluviomarine, are of primary interest to the petroleum industry (Abam & Nwankwoala, 2020). The Akata and Agbada formations provide hydrocarbon source rock and a reservoir and account for almost all the hydrocarbons in the region. The Benin Formation, which occurs at shallower horizons, comprises a continental deposit of sand and gravel (Abam & Nwankwoala, 2020), is important in groundwater exploration.

Materials and methods

Theoretical background

Empirical relations exist that link the aquifer hydraulic properties with electrical properties (George et al., 2015; Ibanga
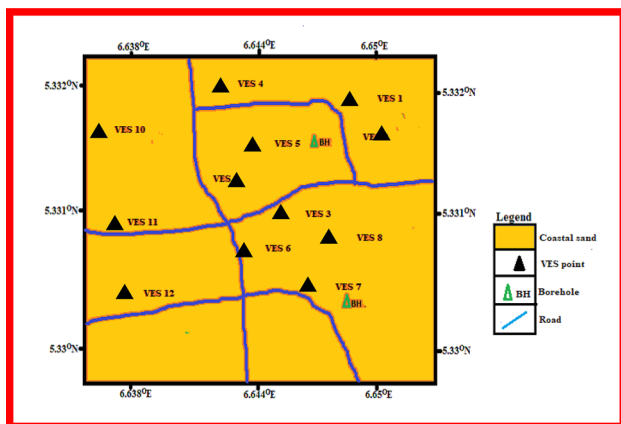

Fig. 1 Geologic map of study area showing VES points

& George, 2016; Ibuot et al., 2017b; Obiora et al., 2018). These relations provide a cost-effective means of deriving aquifer hydraulic properties (hydraulic conductivity, transmissivity, etc.) from surficial resistivity measurements without the need to do any pumping tests which is usually expensive. Archie (1942) developed a model equation that relates the electrical resistivity of rocks/soils and the pore-water resistivity. This relationship can be expressed using Eq. 1 as the quotient of the bulk electrical resistivity (ρ_b) to pore-water resistivity (ρ_w) for a fully saturated and clay-free formation.

$$F = \frac{\rho_b}{\rho_w} \tag{1}$$

where F is the formation factor which represents a macroscopic property of rock/soil. Formation factor as function of the porosity of the rock pore structure, and pore size distribution. The formation factor is affected by factors such as the mineralogy of the rock, the degree of compaction, and the salinity and conductivity of the pore fluid. It is typically reported as a dimensionless number, with lower values indicating more conductive rocks and higher values indicating more resistive rocks (Ekanem et al., 2022).

Considering a water-saturated sediment, porosity which is the percentage of the rock/soil that is void of materials determines the quantity of water an aquifer can hold in storage. Porosity can have a significant impact on the properties and behaviour of a material. Highly porous materials tend to have low density, and high permeability. On the other hand, materials with low porosity tend to have higher density, and lower permeability. Then, effective porosity (ϕ) of a saturated geologic formation can express using Eq. 2.

$$\phi = \left(\frac{a}{F}\right)^{\frac{1}{m}} \tag{2}$$

where a and m are Archie constants, a is the geometric factor ($a = 0.52$) and m is the cementation factor ($m = 1.54$). The conductivity of water saturated rock/soil is very sensitive to changes in either of a or m.

The hydraulic conductivity, K, which is related to porosity was estimated using the Kozeny-Carman-Bear's equation as expressed in Eq. 3. It depends on the pore dynamics of the sand the fluid is flowing through and measures the capacity of a geologic formation or other porous media to transmit fluids. Hydraulic conductivity plays an important role in a wide range of applications, from groundwater flow and contamination studies to civil engineering and soil science.

$$K = \left(\frac{\delta_w \cdot g}{\mu_d}\right) \cdot \left(\frac{d_m^2}{180}\right) \cdot \left(\frac{\phi^3}{(1-\phi)^2}\right) \tag{3}$$

where ϕ is the effective porosity, g is the acceleration due gravity (10 m/s^2), δ_w is the density of water (1000 kg/m^3), d_m is site mean diameter (0.00036 m) measured using the micrometre screw gauge, μ_d is the dynamic viscosity of water which is approximately 0.0014 kg/ms (Fetters, 1994).

The protectivity and potentiality of the aquifer are determined using the Dar Zarrouk parameters (longitudinal conductance and transverse resistance) and transmissivity. The protectivity, which expresses the ability of the overlying layers to retard percolating fluids, is greatly influenced by permeability, soil particle size, porosity, and the thickness of the protecting layers (Adeniji et al., 2014; Ekanem et al., 2021; Obiora et al., 2015).

The product of hydraulic conductivity (K) and thickness (h) gives the values of transmissivity (T_r) which describe the transmitting ability of an aquifer to allow groundwater to move wholly in its saturated thickness. This property is expressed in Eq. 4 according to Niwas and Singhal (1981). Transmissivity rates the ease of an aquifer to transmit water over a unit thickness of hydraulic conductivity and across the entire thickness of the aquifer.

$$T_r = Kh \tag{4}$$

The total longitudinal conductance (S) and transverse resistance (T), which are functions of the first-order geoelectric parameters (resistivity and thickness), were estimated at each VES point using the mathematical relation as given in Eq. 5.

$$S = \sum_i^n \frac{h_i}{\rho_i} \tag{5}$$

$$T = \sum_i^n \rho h \tag{6}$$

where ρ and h are the resistivity and thickness of the overlying layers.

Data acquisition and processing

The electrical resistivity survey was conducted in the study area using the Integrated Geo and Instrument Services (IGIS) signal enhancement resistivity meter with model SSR-MP-ATS and its accessories. The vertical electrical sounding (VES) technique utilizing the Schlumberger electrode configuration was used in acquiring VES data at twelve locations within the study area. The technique involved the injection of current into the earth through a pair of current electrodes (A and B), while a pair of potential electrodes (M and N) measured the potential differences generated. The half-current electrode separation (AB/2) ranged between 1 and 200 m while the potential electrode (MN/2) ranged

between 0.25 and 30 m. The IGIS resistivity meter computed the ratio of potential difference to current as the apparent resistance of the subsurface layers penetrated by the current. The apparent resistance was converted to apparent resistivity using Eq. 7.

$$\rho_a = G.R_a \tag{7}$$

where R_a is the apparent resistance and G is the geometric factor for Schlumberger electrode configuration and is expressed in Eq. 8 as;

$$G = \pi . \left[\frac{\left(\frac{AB}{2}\right)^2 - \left(\frac{MN}{2}\right)^2}{MN} \right] \tag{8}$$

where AB and MN are the current and potential electrodes distances, respectively.

Using the conventional manual curve matching technique, the smoothened VES curves were interpreted to generate the initial values of layer resistivities and thicknesses (Zohdy et al., 1974). The initial values were used as input parameters in a WINRESIST software program, which electronically carried out a least-squares inversion of the field data and gave a resistivity model curve where the true values of resistivity, thickness, and depth at each VES point can be obtained. After a series of iterations, reasonably acceptable variations between the field and theoretical data were realized through the absolute resulting root-mean-square (RMS) error. The best fitting models to the data represent the subsurface resistivity models. Samples of the VES-interpreted resistivity model curves are shown in Figs. 1 and 2. The values of resistivity and thickness of the layers were used in Eqs. 1–6 to derive the geohydraulic properties (formation factor, porosity, hydraulic conductivity, transmissivity, longitudinal conductance, and transverse resistance) and the corrosivity of the topmost layer of the earth from surface resistivity measurements without the need to do any pumping tests, which are usually expensive.
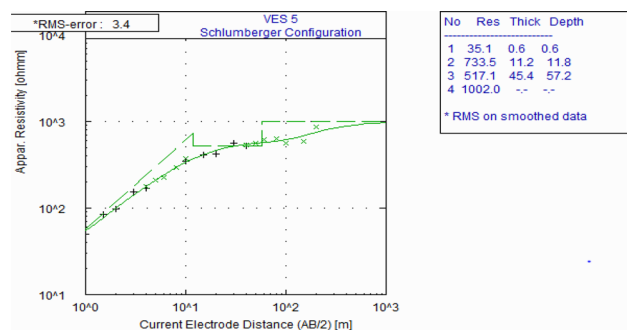

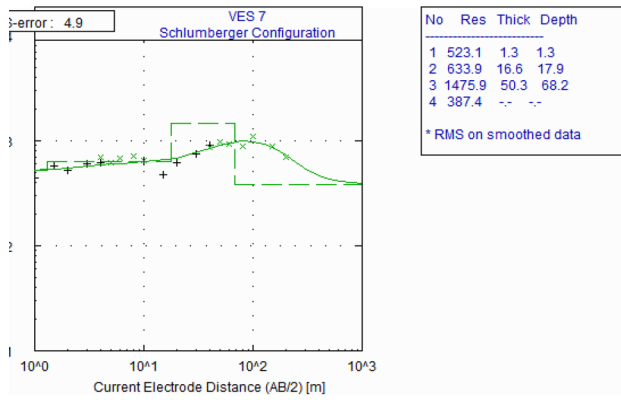**Fig. 2** Model resistivity curve at VES 5

Fig. 3 Model resistivity curve at VES 7

Results and discussion

The interpretation of VES data gives the representative VES curves as shown in Figs. 2 and 3. This led to the realization of the values of the resistivity, thickness, and depth of the geo-electric layers within the maximum current electrode separation presented in Table 1, and four geo-electric layers were delineated in all locations. The first layer which is extensively exposed at the surface has a resistivity range of 35.1–891.6 Ωm, and averages to 415.3 Ωm and was delineated as motley topsoil. The relatively higher resistivity values observed in some locations may be due to the presence of high grain size materials like gravels, coarse sands, breccias and other detrital geomaterials in lithostrata of this layer (Ekanem et al., 2020; George et al., 2015; Ibuot et al., 2013). This layer has thickness and depth that varies from 0.6 to 4.5 m respectively in vertical extent. This geoelectric layer boosts the seapage of fluids into the underlying lithologic units. The second geoelectric layer with resistivity values ranging from 34.1 to 816.8 Ωm averaging about 337.5 Ωm has thickness and depth ranging from 4.1 to 16.6 m and 6.1 to 17.9 m, respectively. The lower resistivity may be attributed to the presence of conductive argillaceous materials and clay intercalations. This layer was delineated as a medium-grained sand dominated by lithostrata, and on average is less resistive than the overlying layer and is also highly permeable. This indicates that the underlying hydrogeologic unit is vulnerable to surface contaminants. Underlying the second layer is the third layer, which was interpreted as a fine-medium grained sand-dominated layer. The resistivity values of the layer vary from 41.6 to 1475.9 Ωm with a mean value of 513.03 Ωm, the thickness and depth of this lithologic layer vary from 9.2 to 50.3 m and 16.8 to 68.2 m, respectively. This was identified as the main hydrogeologic unit with the highest resistivity and thickness observed at VES 7. The fourth layer has variable resistivity spanning from 20.6 to 2645.4 Ωm with thickness and depth not defined

Table 1 Summary of electrical resistivity survey in the study area

VES no.	Longitude (°E)	Latitude (°N)	Elevation (m)	Layer resistivity (Ωm)				Layer thickness (m)			Layer depth (m)			Curve types	Corrosivity
				ρ_1	ρ_2	ρ_3	ρ_4	h_1	h_2	h_3	d_1	d_2	d_3		
1	6.6518	5.3320	18	891.6	111.0	834.7	47.4	2.6	8.8	28.6	2.6	11.4	40.1	HK	PNC
2	6.6519	5.3311	17	525.7	110.6	861.7	11,936.1	4.5	9.7	14.8	4.5	14.2	29.0	HA	PNC
3	6.6517	5.3302	16	425.3	34.1	292.7	20.6	1.8	4.4	13.9	1.8	6.1	20.0	HK	PNC
4	6.6508	5.3296	10	39.7	106.1	41.6	333.4	5.4	9.5	30.5	5.4	14.8	45.4	KH	MC
5	6.6507	5.3307	17	35.1	733.5	517.1	1002.0	0.6	11.2	45.4	0.6	11.8	57.2	KH	MC
6	6.6498	5.3308	14	773.0	816.8	386.3	55.8	1.2	6.5	9.2	1.2	7.6	16.8	KQ	PNC
7	6.6488	5.3305	16	523.1	633.9	1475.9	387.4	1.3	16.6	50.3	1.3	17.9	68.2	AK	PNC
8	6.6495	5.3327	15	555.0	549.3	177.6	2645.4	3.5	7.0	22.5	3.5	10.5	33.0	KH	PNC
9	6.6494	5.3322	13	547.0	643.5	1023.3	12,651.0	1.6	12.0	27.0	1.6	13.6	40.6	AA	PNC
10	6.6506	5.3326	15	120.3	114.7	269.1	176.2	2.0	5.0	22.6	2.0	7.0	29.6	HK	SC
11	6.6373	5.3318	19	170.8	83.2	66.4	111.3	2.0	4.1	21.7	2.0	6.1	27.8	QH	SC
12	6.6492	5.3314	13	376.7	113.6	209.9	263.4	4.4	6.5	30.9	4.4	10.9	41.8	HA	PNC
Average				415.3	337.5	513.03	2469.2	2.6	8.4	26.5	2.6	11.0	37.1		

PNC practically non corrosive, MC mildly corrosive, SC slightly corrosive

within the maximum current electrode separation. The high resistivity values at some locations suggest that this layer is compose of gravelly sand. The result obtained was compared with borehole lithology logs of existing and nearby borehole (Fig. 4) which shows strong correlations.

The variations observed across the subsurface imply the variability in intra-lithological composition of the argillaceous geomaterials (George et al., 2015; Ibuot et al., 2013). The results in Table 1 also reveal the study area to be characterised by the HK, HA, KH, KQ, AK, AA, and QH curve types, and these variations infer changes in subsurface lithologies. Seven curve types were identified, where HK and KH were dominant, with each constituting 25%. HA has a 16.67% composition while KQ, AK, AA, and QH had the least dominance, constituting 8.33%. The distribution of these curve types is displayed in a pie chart and shown in Fig. 5. The utility pipes that convey water are buried in the topmost layer of the earth's subsurface. The resistivity values of this layer were used in assessing the corrosivity potential of this layer. The ratings according to Oladapo et al. (2004) and Mosuro et al. (2017) were employed. The results revealed that VES 1, 2, 3, 6, 7, 8, 9, and 10 were practically noncorrosive (PNC), VES 4 and 5 were observed to be moderately corrosive (MC), while VES 10 and 11 were slightly corrosive (SC). Areas that are practically noncorrosive (PNC) are good for the burying of underground metal pipes without corrosion. Areas that are slightly and moderately corrosive have low potential for corroding pipes, rupturing or causing leakage of underground metal pipes (Ibuot et al., 2017b; Obiora et al., 2015; Umar & Igwe, 2019). This may be due to ferruginous substances in the geomaterials of the topsoil. The percentage distribution of corrosivity of the topmost layer is shown in Fig. 6, where 66.67% represents PNC while 16.67% represents MC and SC.
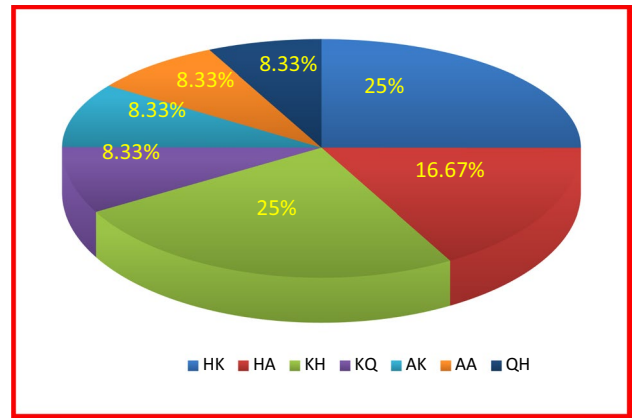

Fig. 4 Borehole lithology and inferred layers at VES 5 and VES 7

Fig. 5 Percentage distribution of the curve types

The primary geoelectric indices (resistivities and thicknesses) were used in estimating the secondary geoelectric indices (formation factor, porosity, hydraulic conductivity, transmissivity, longitudinal conductance, and transverse resistance) presented in Table 2. The resistivity and thickness of the saturated units (aquifer) vary from 41.6 to 1475.9 Ωm and 9.2 to 50.3 m, respectively. The variation of resistivity in this layer may is influenced by the nature of the subsurface geomaterials and the continuous bioturbating activities (Ekanem et al., 2021; Thomas et al., 2020). The pore-water resistivity (ρ_w) has values ranging from 47.5 1083.4 Ωm with an average of 359.77 Ωm, and Fig. 7a and b shows the distributions of bulk aquifer resistivity and pore-water resistivity. There is similarity in the variational trends as an increase in one lead to a corresponding increase in the other. The southern zone of the mapped area shows high values for both parameters. It can be deduced that an area with high bulk resistivity is more saturated with pore water in its repositories. The result of the resistivity values could be affected by the nature of the subsurface geomaterials and the electrical resistivity of the subsurface, according to researchers (Ekanem et al., 2021; George et al., 2015; Ibuot et al.
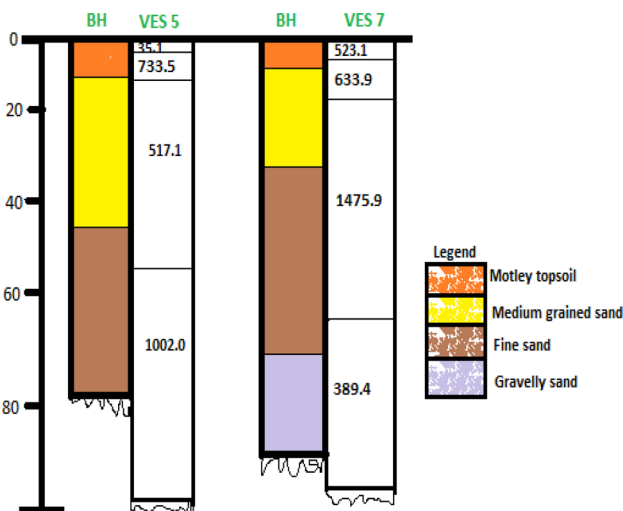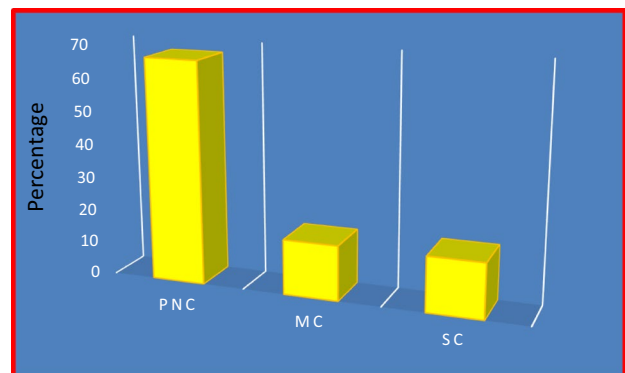

Fig. 6 Percentage distribution of the corrosivity

Table 2 Results of the estimated geohydraulic properties

VES no.	Long. (°E)	Lat. (°N)	Elevation (m)	ρ_a (Ωm)	h_a (m)	ρ_w (Ωm)	F	ϕ	K (m/day)	Tr (m²/day)	S Ω⁻¹	T Ωm²	Aquifer protection rating
1	6.6518	5.3320	18	834.7	28.6	523.6	1.59	0.48	0.0022	0.0629	0.0113	11,429.64	Poor
2	6.6519	5.3311	17	861.7	14.8	188.7	4.57	0.24	0.0001	0.0019	0.0223	9026.94	Poor
3	6.6517	5.3302	16	292.7	13.9	680.3	0.43	1.13	0.4333	6.0229	0.0135	2848.28	Poor
4	6.6508	5.3296	10	41.6	30.5	76.9	0.54	0.98	7.4027	225.7824	0.1022	2172.42	Poor
5	6.6507	5.3307	17	517.1	45.4	427.4	1.21	0.58	0.0056	0.2542	0.0154	9069.48	Poor
6	6.6498	5.3308	14	386.3	9.2	269.3	1.44	0.52	0.0031	0.0285	0.0048	12,241.46	Poor
7	6.6488	5.3305	16	1475.9	50.3	1083.4	1.36	0.54	0.0036	0.1811	0.0155	20,710.30	Poor
8	6.6495	5.3327	15	177.6	22.5	271.7	0.65	0.86	0.1725	3.8813	0.0095	11,595.15	Poor
9	6.6494	5.3322	13	1023.3	27.0	364.9	2.80	0.34	0.0004	0.0108	0.0114	16,190.80	Poor
10	6.6506	5.3326	15	269.1	22.6	136.8	1.97	0.42	0.0012	0.0271	0.0298	1645.00	Poor
11	6.6373	5.3318	19	66.4	21.7	47.5	1.40	0.53	0.0033	0.0716	0.0240	1549.40	Poor
12	6.6492	5.3314	13	209.9	30.9	138.7	1.51	0.50	0.0026	0.0803	0.0222	5344.27	Poor
Average				513.02	26.45	350.77	1.62	0.59	0.6692	19.7004	0.0235	8651.93	

2021; Uwa et al., 2018). It is affected by the density, shape, size, pore size, and porosity of the constituent geomaterials; lithology; water content; clay content; and salinity.

The study area has topographic elevations that range from 10 to 19 m with an average of 13 m, indicating a low-lying region. The image map (Fig. 8) shows the lowest elevation in the southeastern zone of the mapped area. This implies that water flows from topographically high regions to topographically low regions (southeastern region), and can predict the direction of flow of contaminants (Ekanem et al., 2021; Ibuot et al., 2019a, 2019b). The formation factor is estimated from Eq. 1 as the ratio of bulk resistivity to water resistivity, whose range and mean are 0.43–4.57 and 1.62, respectively. The spatial variation of the formation factor is displayed in the image map (Fig. 9). According to Ekanem et al. (2020), the formation factor is sensitive to pore-fluid and lithogical textures. Regions with high values of formation factor may be inferred as regions with more resistive rocks. The effective porosity, which depends on the grain composition of the soil, the way it is formed and the pressure to which it is exposed (Halek and Svec, 1979), has values ranging from 0.24 to 1.13 with a mean value of 0.59. The image map (Fig. 10) displayed the variation of porosity across the study area. The regions with high porosity may be delineated as regions having low density and high permeability. It is observed from Figs. 9 and 10 that the values of formation factor increase at locations where values of porosity decrease. This may be attributed to high argillite-sand mixing ratios that reduce pore-matrix ratios in aquifers.

Hydraulic conductivity is a geoelectrical parameter that measures the ease with which saturated soil pores allow water to move. The estimated hydraulic conductivity range and mean are 0.0001–7.4027 m/day and 0.6692 m/day respectively. Figure 11 shows the distribution of hydraulic conductivity where a zone with a high magnitude of hydraulic conductivity is observed in the southeastern part of the study area. This zone with relatively high hydraulic conductivity indicates a zone with high permeability and high groundwater transmissibility (Ekanem et al., 2022; Vázquez-Báez et al., 2019). The zone with high hydraulic conductivity can be delineated as zone with high water availability and rapid groundwater recharge. The variation may be attributed to the existence of dead-end pores as a result of residual argillites in the tortuous path (George et al., 2015). The aquifer transmissivity varies from 0.0019 to 225.7824 with a mean of 19.7004; this parameter is important in determining the ability of a saturated thickness to allow fluid (groundwater) to pass through its entire thickness. It is a function of hydraulic conductivity and thickness. The image map (Fig. 12) depicts the distribution of transmissivity, which follows the same trend as hydraulic conductivity (Fig. 11). This implies that an increase in hydraulic conductivity leads to a corresponding increase in transmissivity.
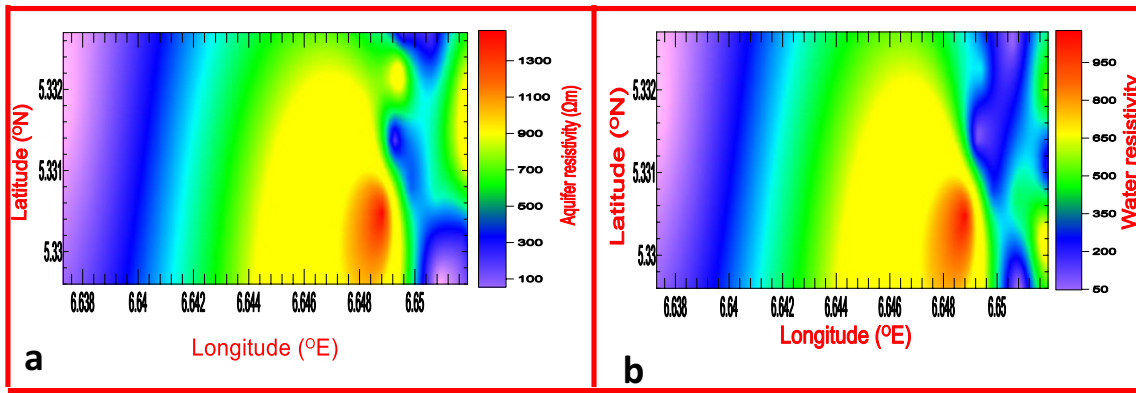
Fig. 7 **a** Distribution of aquifer resistivity **b** distribution of water resistivity
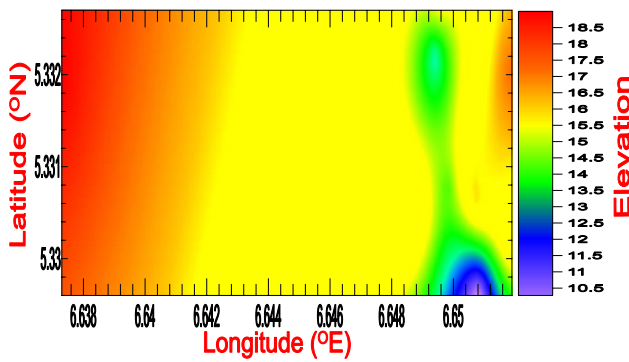

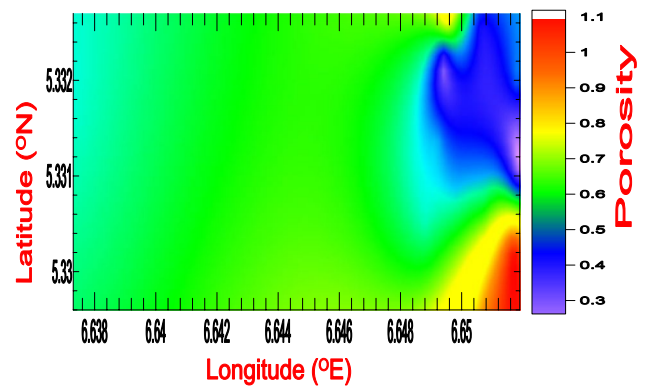**Fig. 8** 2-D image showing distribution of elevation

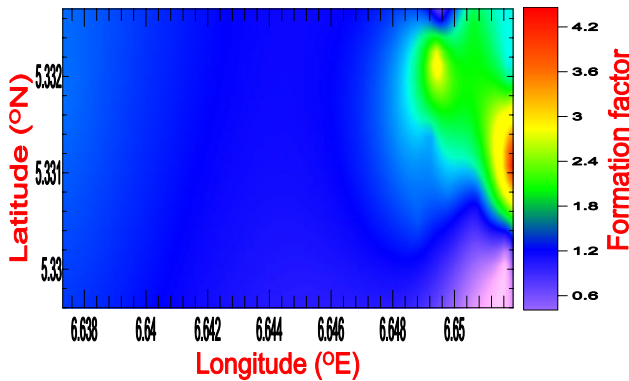**Fig. 10** 2-D image map showing variation of porosity

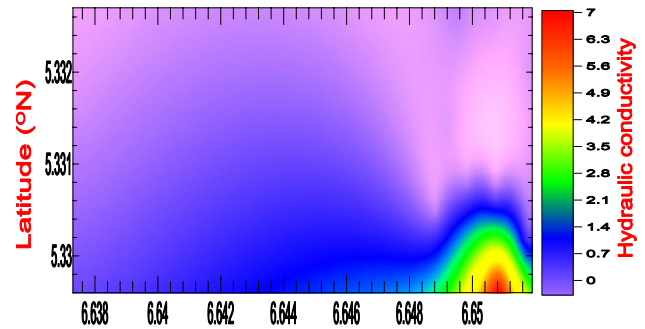**Fig. 9** 2-D image map showing variation of formation factor

Fig. 11 2-D image map showing the distribution of hydraulic conductivity

To assess the protective capacity of the aquifer, the inferred resistivities and thicknesses were used to estimate the longitudinal conductance. The estimated values range from 0.0048 to 0.1022 Ω^{-1} with an average of 0.0235 Ω^{-1}, with aid in classifying the aquifer protective capacity of the study area based on the rating in Table 3 (Abiola et al., 2009; Henriet, 1976). The result revealed that the study area has generally poor protective capacity. This implies that the

entire study area is susceptible to contaminants percolating into the subsurface, so pollutants may more easily enter the groundwater repositories. This can result in the contamination of drinking water wells/boreholes, which can have serious health implications. Figure 13 displays the distribution of longitudinal conductance across the study area.

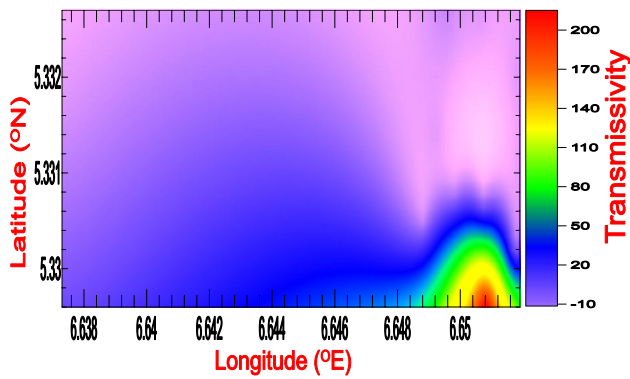The estimated transverse resistance has values ranging from 1549.40 to 20,710.30 Ωm^2 and a mean of 8651.93 Ωm^2. The

Fig. 12 2-D image map showing the distribution of transmissivity

Fig. 14 2-D image map showing the distribution of transverse resistance

Table 3 Longitudinal conductance (mho) and aquifer protective capacity rating (Abiola et al., 2009; Henriet, 1976)

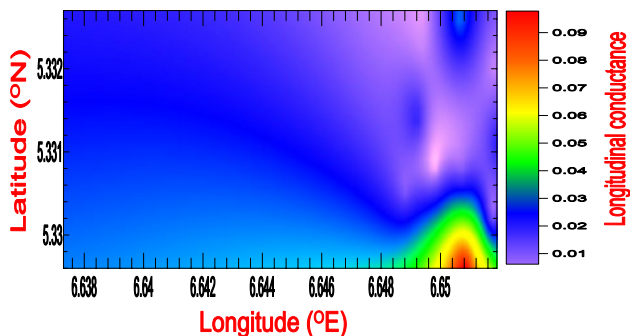| Longitudinal conductance (mhos)	Protective capacity rating
> 10	Excellent
5–10	Very good
0.7–4.49	Good
0.2–0.69	Moderate
0.1–0.19	Weak
< 0.1	Poor

Fig. 13 2-D image map showing the distribution of longitudinal conductance

distribution (Fig. 14) of this parameter revealed the variational trend in the size and potential of groundwater in the study area. An increase in resistivity translates to a corresponding increase in transverse resistance.

Conclusion

The study was carried out to assess the aquifer repositories, protective capacity, and corrosivity employing the surficial electrical resistivity method. The result revealed the study
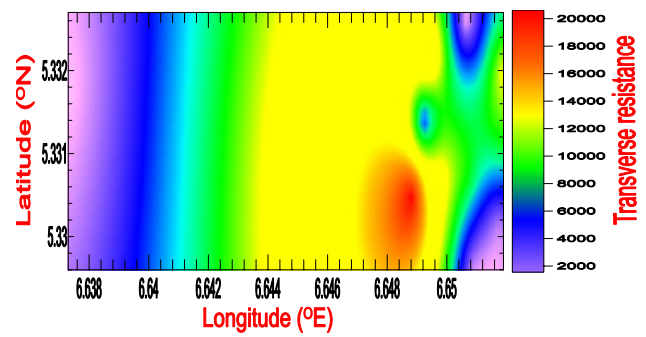
area to be characterized by four geo-electrical layers with inferred layer resistivities, thicknesses, and depths constrained by borehole geological information. The third layer, with a resistivity range of 41.6–1475.9 Ωm, was delineated as the aquifer unit in all the VES locations, with thickness ranging from 9.2 to 50.3 m. The geohydraulic parameters (formation factor, hydraulic conductivity, porosity, transmissivity, longitudinal conductance, and transverse resistance) were estimated using modelled equations and their spatial distributions are displayed in the image maps. The fine-to-medium grained sand that characterized the aquifer units revealed the prolific groundwater potential of the study area. Greater part of the study area is poorly protected, this implies that groundwater in the area is likely polluted by some materials percolating through the overlying layers. This can have serious implications for both human and environmental health, as well as economic and social well-being. The corrosivity rating of the top soil indicates that it is practically noncorrosive (PNC), moderately corrosive (MC), and slightly corrosive (SC), with PNC accounting for 66.67% and MC and SC accounting for 16.67%. The protective capacity rating revealed that the study area is generally poorly protected. This implies that the groundwater in the area is prone to contamination due to the high permeability of the protective layers. The result of this study is very promising as it provides useful information that will help in groundwater exploitation, development, and management.

Data availability statement All relevant data are included in the paper or its supplementary information.

Declarations

Conflict of interest The authors declare that they have no conflicts of interest.

References

Abam, T. K. S., & Nwankwoala, H. O. (2020). Hydrogeology of Eastern Niger Delta: A review. *Journal of Water Resource and Protection, 12*, 741–777.

Abiola, O., Enikanselu, P. A., & Oladapo, M. I. (2009). Groundwater potential and aquifer protective capacity of overburden units in Ado-Ekiti, southwestern Nigeria. *International Journal of Physical Sciences, 4*(3), 120–132.

Adeniji, A. E., Omonona, O. V., Obiora, D. N., & Chukudebelu, J. U. (2014). Evaluation of soil corrosivity and aquifer protective capacity using geoelectrical investigation in Bwari basement area; Abuja. *Journal of Earth System Science, 123*, 491–502.

Akpan, A. E., Ugbaja, A. N., & George, N. J. (2013). Integrated geophysical, geochemical and hydrogeological investigation of shallow groundwater resources in parts of the Ikom-Mamfe Embayment and the adjoining areas in Cross River State, Nigeria. *Environmental Earth Sciences, 70*(3), 1435–1456.

Aleke, C. G., Ibuot, J. C., & Obiora, D. N. (2018). Application of electrical resistivity method in estimating geohydraulic properties of a sandy hydrolithofacies: A case study of Ajali Sandstone in Ninth Mile, Enugu State, Nigeria. *Arabian Journal of Geosciences, 11*, 322.

Archie, G. E. (1942). The electrical resistivity log as an aid in determining some reservoirs characteristic grain. *AIME, 146*, 54–62.

Bashir, I. Y., Izham, M. Y., & Main, R. (2014). Vertical electrical sounding investigation of aquifer composition and its potential to yield groundwater in some selected Towns in Bida basin of North central Nigeria. *Journal of Geography and Geology, 6*(1), 60–69.

Bayewu, O. O., Oloruntola, M. O., Mosuro, G. O., Laniyan, T. A., Ariyo, S. O., & Fatoba, J. O. (2018). Assessment of groundwater prospect and aquifer protective capacity using resistivity method in Olabisi Onabanjo University campus, Ago-Iwoye, Southwestern Nigeria. *NRIAG Journal of Astronomy and Geophysics, 7*, 347–360.

Bricker, S. H., Banks, V. J., Galik, G., Tapete, D., & Jones, R. (2017). Accounting for groundwater in future city visions. *Land Use Policy, 69*, 618–630.

Daniel, E. O., Ibuot, J. C., Ugbor, D. O., & Obiora, D. N. (2022). Spatial analysis and modeling of litho- exutural properties of hydrogeological units in Ofu Local Government Area of Kogi State, North-Central, Nigeria. *Modeling Earth Systems and Environment*. https://doi.org/10.1007/s40808-022-01645-7.

Ekanem, A. M., Akpan, A. E., George, N. J., & Thomas, J. E. (2021). Appraisal of protectivity and corrosivity of surficial hydrogeological units via geo-sounding measurements. *Environmental Monitoring and Assessment, 193*, 718. https://doi.org/10.1007/s10661-021-09

Ekanem, A. M., George, N. J., Thomas, J. E., & Nathaniel, E. U. (2020). Empirical relations between aquifer geohydraulic-geoelectric properties derived from surfcial resistivity measurements in parts of Akwa Ibom State, Southern Nigeria. *Natural Resources Research, 29*(4), 2635–2646.

Ekanem, K. R., George, N. J., & Ekanem, A. M. (2022). Parametric characterization, protectivity and potentiality of shallow hydrogeological units of a medium-sized housing estate, Shelter Afrique, Akwa Ibom State, Southern Nigeria. *Acta Geophysica*. https://doi.org/10.1007/s11600-022-00737-3

Fetter, C. W. (1994). *Applied hydrogeology* (3rd ed.). Macmillan College Publishing Company.

George, J. N., Ibuot, J. C., & Obiora, D. N. (2015). Geoelectrohydraulic of shallow sandy in Itu, Akwa Ibom State (Nigeria) using geoelectric and hydrogeological measurements. *Journal of African Earth Sciences, 110*, 52–63.

George, N. J. (2020). Appraisal of hydraulic flow units and factors of the dynamics and contamination of hydrogeological units in the littoral zones: a case study of Akwa Ibom State University and its Environs, Mkpat Enin LGA, Nigeria. *Natural Resources Research*. https://doi.org/10.1007/s11053-020-09673-9

George, N. J., Ubom, A. I., & Ibanga, J. I. (2014). Integrated approach to investigate the effect of leachate on groundwater around the Ikot Ekpene Dumpsite in Akwa Ibom State, Southeastern Nigeria. *International Journal of Geophysics*. https://doi.org/10.1155/2014/174589

George, N. J., Umoh, J. A., Ekanem, A. M., Agbasi, O. E., Asfahani, J., & Thomas, J. E. (2022). Geophysical-laboratory data integration for estimation of groundwater volumetric reserve of a coastal hinterland through optimized interpolation of interconnected geopore architecture. *Journal of Coastal Conservation*. https://doi.org/10.1007/s11852-022-00902-2

Halek, V., & Svec, J. (1979). *Groundwater Hydraulics*. New York: Elsevier Scientific Publishing Company.

Henriet, J. P. (1976). Direct application of the Dar Zarrouk parameters in groundwater, surveys. *Geophysical Prospecting, 24*, 334–353.

Hossain, M. L., Das, S. R., & Hossain, M. K. (2014). Impact of landfill leachate on surface and groundwater quality. *Journal of Environmental Science and Technology, 7*, 337–346.

Ibanga, J. I., & George, N. J. (2016). Estimating geohydraulic parameters, protective strength, and corrosivity of hydrogeological units: A case study of ALSCON, Ikot Abasi, southern Nigeria. *Arabian Journal of Geoscience, 9*, 363.

Ibuot, J. C., Aka, M. U., Inyang, N. J., & Agbasi, O. E. (2022). Georesistivity and physicochemical evaluation of hydrogeologic units in parts of Akwa Ibom State, Nigeria. *International Journal of Energy and Water Resources*. https://doi.org/10.1007/s42108-022-00191-3

Ibuot, J. C., Akpabio, G. T., & George, N. J. (2013). A survey of the repository of groundwater potential and distribution using geoelectrical resistivity method in Itu Local Government Area (LGA), Akwa Ibom State, southern Nigeria. *Central European Journal of Geosciences, 5*(4), 538–547.

Ibuot, J. C., George, N. J., Okwesili, A. N., & Obiora, D. N. (2019a). Investigation of litho-textural characteristics of aquifer in Nkanu West Local Government Area of Enugu state, southeastern Nigeria. *Journal of African Earth Sciences, 157*(2019), 197–207.

Ibuot, J. C., & Obiora, D. N. (2021). Estimating geohydrodynamic parameters and their implications on aquifer repositories: A case study of University of Nigeria, Nsukka, Enugu State. *Water Practice and Technology, I6*(1), 162–181.

Ibuot, J. C., Obiora, D. N., Ekpa, M. M., & Okoroh, D. O. (2017b). Geoelectrohydraulic Investigation of the surfcial aquifer units and corrosivity in parts of Uyo L. G. A., AkwaIbom, Southern Nigeria. *Journal of Applied Water Science, 7*, 4705–4713.

Ibuot, J. C., Okeke, F. N., George, N. J., & Obiora, D. N. (2017a). Geophysical and physicochemical characterization of organic waste contamination of hydrolithofacies in the coastal dumpsite of Akwa Ibom State, Southern Nigeria. *Water Science and Technology: Water Supply, 17*(6), 1626–1637.

Ibuot, J. C., Okeke, F. N., Obiora, D. N., & George, N. J. (2019b). Assessment of impact leachate on hydrogeological repositories in Uyo, Southern Nigeria. *Journal of Environmental Engineering and Science, 14*(2), 97–107.

Ibuot, J. C., Omeje, E. T., & Obiora, D. N. (2021). Geophysical evaluation of geohydrokinetic properties of aquifer units in parts of Enugu state. *Nigeria. Water Practice and Technology, 16*(4), 1397–1409.

Lahjouj, A., El Hmaidi, A., Bouhafa, K., & Boufala, M. (2020). Mapping specifc groundwater vulnerability to nitrate using random forest: case of Sais basin, Morocco. *Modeling Earth Systems and Environment*. https://doi.org/10.1007/s40808-020-00761-6

Loke M. H. (2009). Electrical imaging surveys for environmental and engineering studies, a guide to 2D and 3D surveys. Workshop held in USM.

Mogaji, K. A., Omosuyi, G. O., & Olayanju, G. M. (2011). Groundwater system evaluation and protective capacity of overburden material at Ile-olujI, Southwestern Nigeria. *Journal of Geology and Mining Research, 3*(11), 294–304.

Mosuro, G. O., Omosanya, K. O., Bayewu, O. O., Oloruntola, M. O., Laniyan, T. A., Atobi, O., Okubena, M., Popoola, E., & Adekoya, F. (2017). Assessment of groundwater vulnerability to leachate infiltration using electrical resistivity method. *Applied Water Science, 7*, 2195–2207. https://doi.org/10.1007/s13201-016-0393-4

Niwas, S., & Singhal, D. C. (1981). Estimation of aquifer transmissivity from Dar Zarrouk parameters in porous media. *Hydrology, 50*, 393–399.

Nugraha, G. U., Bakti, H., Lubis, R. F., Sudrajat, Y., & Arisbaya, I. (2021). Aquifer vulnerability in the Coastal Northern Part of Lombok Island Indonesia. *Environment, Development and Sustainability*. https://doi.org/10.1007/s10668-021-01459-0

Obiora, D. N., Ajala, A. E., & Ibuot, J. C. (2015). Evaluation of aquifer protective capacity of overburden units and soil corrosivity in Makurdi, Benue State, Nigeria, using electrical resistivity method. *Journal of Earth System Science, 124*(1), 125–135.

Obiora, D. N., & Ibuot, J. C. (2020). Geophysical assessment of aquifer vulnerability and management: A case study of University of Nigeria, Nsukka, Enugu State. *Applied Water Science, 10*, 29. https://doi.org/10.1007/s13201-019-1113-7

Obiora, D. N., Ibuot, J. C., Alhassan, U. D., & Okeke, F. N. (2018). Study of aquifer characteristics in northern Paiko, Niger State, Nigeria, using geoelectric resistivity method. *International Journal of Environmental Science and Technology, 15*(11), 2423–2432.

Obiora, D. N., Ibuot, J. C., & George, N. J. (2016). Evaluation of aquifer potential, geoelectric and hydraulic parameters in Ezza north, Southeastern Nigeria, using geoelectric sounding. *International Journal of Environmental Science and Technology, 13*(2), 435–444.

Oladapo, M. I., Mohammed, M. Z., Adeoye, O. O., & Adetola, O. O. (2004). Geoelectric investigation of the Ondo State Housing Corporation Estate; Ijapo, Akure, Southwestern Nigeria. *Journal of Mining and Geology, 40*, 41–48.

Omeje, E. T., Obiora, D. N., Okeke, F. N., Ibuot, J. C., & Ugbor, D. O. (2023). Investigation of aquifer vulnerability and sensitivity analysis of modified drastic and sintacs models: a case study of Ovogovo Area, Eastern Nigeria. *Acta Geophysica*. https://doi.org/10.1007/s11600-022-00992-4

Opara, A. I., Eke, D. R., Onu, N. N., Ekwe, A. C., Akaolisa, A. C., Okoli, A. E., & Inyang, G. E. (2020). Geo-hydraulic evaluation of aquifers of the Upper Imo River Basin, Southeastern Nigeria using Dar-Zarrouk parameters. *International Journal of Energy and Water Resources*. https://doi.org/10.1007/s42108-020-00099-w

Oseji, J. O., Egbai, J. C., Okolie, E. C., & Ese, E. C. (2018). Investigation of the Aquifer Protective Capacity and Groundwater Quality around Some Open Dumpsites in Sapele Delta State, Nigeria. *Hindawi Applied and Environmental Soil Science*. https://doi.org/10.1155/2018/365302

Putranto, T. T., Santi, N., Dian Agus Widiarso, D. A., & Dimas Pamungkas, D. (2018). Application of aquifer vulnerability index (AVI) method to assess groundwater vulnerability to contamination in Semarang urban area. *MATEC Web of Conferences Series, 159*, 01036.

Tamunobereton-ari, I., Omubo-Pepple, V. B., & Amakiri, A. R. C. (2014). Characterization and delineation of aquifer in part of Omoku, Rivers State, Nigeria. *IOSR Journal of Applied Geology and Geophysics, 2*(4), 30–37.

Thomas, J. E., George, N. J., Ekanem, A. M., & Nsikak, E. E. (2020). Electrostratigraphy and hydrogeochemistry of hyporheic zone and water-bearing caches in the littoral shorefront of Akwa Ibom State University, Southern Nigeria. *Environmental Monitoring and Assessment, 192*, 505. https://doi.org/10.1007/s10661-020-08436-6

Umar, N. D., & Igwe, O. (2019). Geo-electric method applied to groundwater protection of a granular sandstone aquifer. *Applied Water Science*. https://doi.org/10.1007/s13201-019-0980-2

Uwa, U. E., Akpabio, G. T., & George, N. J. (2018). Geohydrodynamic Parameters and Their Implications on the Coastal Conservation: A Case Study of Abak Local Government Area (LGA), Akwa Ibom State, Southern, Nigeria. *Natural Resources Research*. https://doi.org/10.1007/s11053-018-9391-6

Vázquez-Báez, V., Rubio-Arellano, A., & García-Toral, R. M. I. (2019). Modeling an aquifer numerical solution to the groundwater fow equation. *Mathematical Problems in Engineering*. https://doi.org/10.1155/2019/1613726

Zohdy, A. A. R., Eaton, G. P., & Mabey, D. R. (1974). Application of surface geophysics to groundwater investigation. *USGS Techniques of Water Resources Investigations*. https://doi.org/10.3133/twri02D1